Monodisperse colloidal plates under shear

A. B. D. Brown*
Semiconductor Physics, Cavendish Laboratory, Madingley Road, Cambridge CB3 0HE, United Kingdom

A. R. Rennie†
Department of Chemistry, Kings College London, Strand, London WC2R 2LS, United Kingdom
(Received 16 August 1999; revised manuscript received 6 December 1999)

The structure of a dispersion of monodispersed, plate-shaped colloidal particles has been investigated under shear. The dispersion displays a columnar phase when at rest, and if subjected to shear at low rates ($0.1–1\ s^{-1}$), this structure aligns with the axis of the columns in the flow direction. At low shear rates, the plates within these columns are tilted, with their normals in the compressional quadrant, at 20° to the flow direction in the flow-gradient plane. At high shear rates ($\sim 100\ s^{-1}$), the dispersion forms a different structure that consists of layers of particles with their plate normals in the gradient direction. The transition between these two shear-induced ''phases'' is described. Evidence is presented that suggests that at intermediate shear rates there is coexistence between the two phases, implying that there is a shear-induced ''phase separation.'' As the shear rate is further increased evidence for shear-induced disorder is found. All the shear-induced structures that have been observed relax back to the equilibrium columnar phase over a period of a few hours. At rest after shear at low rates ($0.1–1\ s^{-1}$), the amount of orientational order present in the aligned columnar phase increases, while there is no measurable positional rearrangement. After shear at high rates ($67–1000\ s^{-1}$), the layer phase relaxes into a columnar phase. The structure changes via an intermediate state consisting of planes of particles normal to the vorticity direction. The positional rearrangement occurs at the expense of the orientational order, which increases again after the positional rearrangement is complete. The final orientation of the columnar phase is such that the direction of alignment of the plates does not change upon relaxation.

PACS number(s): 82.70.Dd, 83.10.Pp, 83.20.Hn, 83.50.Ax

I. INTRODUCTION

The applications of colloidal dispersions frequently require specific rheological properties. Properties of materials formed from colloids may also depend crucially on the structure induced in processing conditions. An understanding of the inter-relation of the structure of dispersions and their rheological properties is therefore of considerable practical importance. At a fundamental level, there has been much recent interest in the physics associated with the structure of model systems under flow [1–7] and the comparison of this information with computer simulations [8–10] and rheological measurements. Colloidal dispersions have been used as models of simple fluids with the advantage that the interactions between the particles can be controlled [4]. This analogy must be treated with care as there will often be a delicate balance between Brownian forces and other interparticle interactions such as the effects of hydrodynamic forces [9,11]. Some features of colloid rheology are well established [12]: there is usually a range of shear rates where the viscosity of a colloidal dispersion falls with increasing shear rate. At higher shear rates, some materials display regimes where the viscosity is constant and then increases catastrophically with shear rate. The origins of the macroscopic stress are the forces between the particles. These forces, in turn, are related to the spatial arrangement of the particles within the dispersion and the way in which these particles interact.

This paper reports an experimental study of the changes observed under shear in a dispersion of nickel (II) hydroxide particles. These are highly monodisperse and have only short-range interparticle interactions. Previous work has shown that these plates form a columnar phase at high concentrations [13,14]. The phase behavior of dispersions of plates at rest has been predicted as a function of particle concentration and aspect ratio from computer simulations [15,16]. This paper is concerned with the changes in structure of concentrated dispersions under steady shear and the temporal evolution of structure when shear stops. Investigation by a combination of small-angle neutron scattering (SANS) and neutron diffraction permits detailed structural studies. The neutron diffraction provides a simple unambiguous measure of the average orientation distribution of crystalline particles. The SANS data can then be used to determine the spatial arrangement of the particles. The principles of these techniques have been described previously [4,17,18]. These methods present a further advantage in the study of rheology in that they do not, themselves, further perturb the sample. Thus they are ideal for studying relaxation processes in model fluids of particles with ''hard'' interactions.

II. BACKGROUND

In colloidal dispersions of spherical particles, shear-induced structures have been extensively studied. Shear has been observed to orient colloidal crystals of electrostatically

*FAX: +44 1223 337271. Electronic address: abdb1@cus.cam.ac.uk

†Author to whom correspondence should be addressed. FAX: +44 20 7848 2810. Electronic address: rennie@colloids.ch.kcl.ac.uk

stabilized particles and to cause domains to grow [1,2]. The structures are observed to promote slip along particular planes and, at high shear rates, to disorder or melt [2,3]. Dispersions of spherical particles that are not crystalline in the absence of shear due to the nature of the particle interactions (e.g., with short-range steric interactions), the concentration of the dispersion, or the range of particle sizes present typically display more subtle structural changes under shear [4,5].

A number of studies of anisotropic particles under shear have been reported [17–22]; however, none of these studies has investigated dispersions that display a highly ordered structure at rest. For example, studies of clays under flow using neutron diffraction [17,18,23] and x-ray diffraction [21] have been described. This has been due to the difficulties involved in preparing and stabilizing dispersions of anisotropic colloidal particles that are sufficiently uniform in size and shape. In this paper, the effect of shear on a dispersion of ordered platelike particles is investigated, and the observed shear-induced structures are described. The phase behavior of platelike particles at rest [13,14,24] can be compared with the results of computer simulations [15,16], but no direct comparison is yet possible with the few simulations of the flow of concentrated anisotropic particles [25,26].

Traditionally, the size, shape, orientation, and interparticle correlation in colloidal dispersions have been investigated using small-angle scattering. For dispersions of monodispersed spherical particles, where the form factor is spherically symmetrical, small-angle scattering yields almost unambiguous data about the spatial arrangement of particle centers. Anisotropic particles display two types of order: positional correlation and orientational alignment. Small-angle scattering contains information about both these types of orders; however, often it is not easy to interpret the scattering pattern. In this paper, a diffraction technique [17,18] is used to complement small-angle neutron scattering and this allows the orientational order to be deduced from the measurements independently from the positional order.

III. EXPERIMENT

A. Preparation of the colloidal dispersions

Dispersions of nickel (II) hydroxide particles were prepared as described previously [13,14]. The particles were hexagonal plates with a thickness of ~10 nm and a diameter of 84 nm ± 13%. The particles were stabilized with a low molecular mass polyacrylate [27]. This provides a uniform surface and a short-range repulsive force that keeps the dispersion stable, and the long-range electrostatic forces are screened by adding electrolyte. Uncertainty in the thickness of the polymer layer and hence the total range of the particle interactions makes it difficult to define and calculate the volume fraction accurately. Hence the concentration of the dispersions will be described in this paper as a weight fraction. The samples used in the shear experiments were all dispersed in 90% D_2O and 10% H_2O. This reduces the incoherent scattering from protons in H_2O and also partially matches the scattering density of the nickel (II) hydroxide, and so reduces the amount of multiple scattering in the SANS measurements. For the sake of simplicity and to enable comparison with previous papers [13,14], the weight fractions quoted in this paper are what the weight fraction would have been were the particles suspended in H_2O.

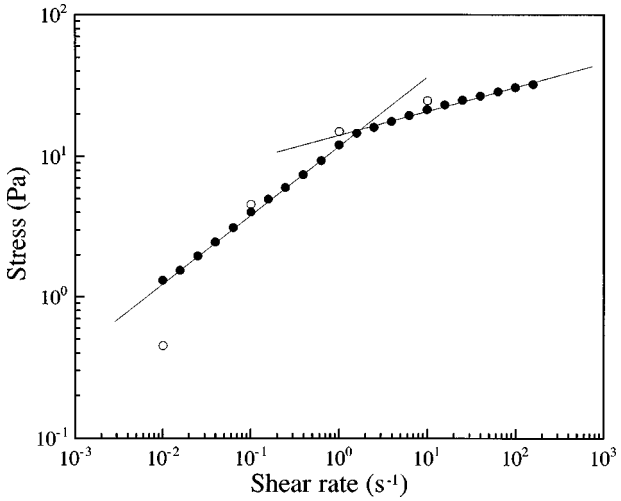

FIG. 1. Variation of stress with shear rate. ●, 10 s shear and then 10 s measurement at each point after preshear at 100 s^{-1}. ○, final stress after half an hour shear at each point.

Under static conditions, such dispersions have been observed to phase separate over a number of days into a columnar phase and a less ordered phase [14]. The particle concentration at which this phase transition occurs depends upon the amount of added electrolyte. It is perhaps most informative to describe the concentration of the samples in relation to this phase separation. For this reason, the position of each sample within the phase separation regime is given as the percentage of the sample volume that would consist of the more ordered phase were the sample left to equilibrate for a number of days. It should be noted that phase separation under static conditions takes between 10 and 40 days, and so when the samples are placed in the shear cell for investigation under shear, they are not separated into two distinctly separate regions of different concentrations. At no point during these experiments on the colloid under shear is macroscopic phase separation observed visually.

B. Rheology

The effective viscosity was measured with cone-plate geometry on a controlled strain rheometer (Rheometrics RDS2) at a number of shear rates. Figure 1 shows the variation of the stress with shear rate. A preshear of 100 s^{-1} was applied before the first series of measurements was taken. These measurements were taken by shearing for 10 s and then by measuring for 10 s. The points were measured from low shear to high shear. To emulate the neutron experiments as much as possible, the sample was then sheared at a constant rate for approximately half an hour and the final stress was taken at each of four shear rates.

The curve is in good agreement with the stresses measured after half an hour of shear at each shear rate, with the exception of the point at 0.01 s^{-1}. This disagreement could be due to the fact that in the first series of measurements, the strain that the sample was subjected to at this shear rate was only 0.1, which was probably not sufficient to destroy whatever structure may have been present in the sample from its shear history. If the data of Fig. 1 are plotted as viscosity

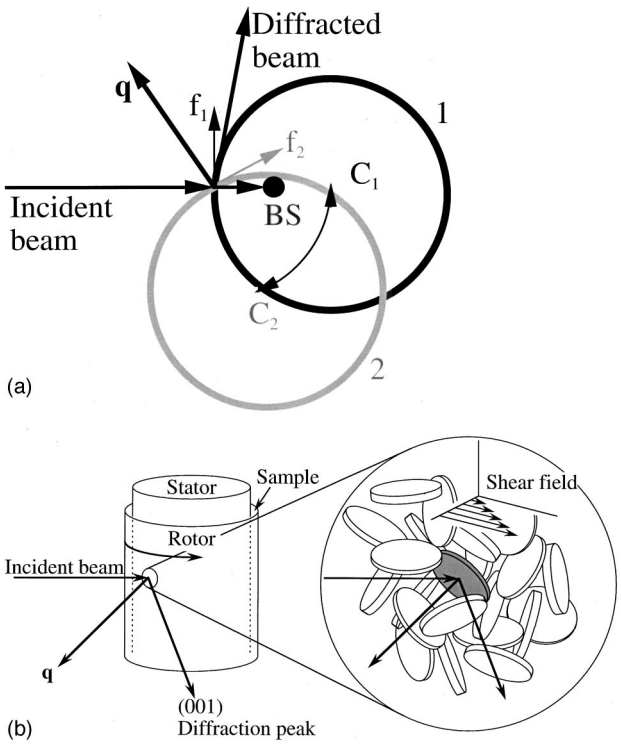

FIG. 2. (a) Two positions of the Couette cell in plan view are shown. In position 1, shown in black, the center of the Couette cell is at C_1 and the flow direction is shown by f_1. In position 2, shown in gray, the center of the Couette cell is at C_2 and the flow direction is shown by f_2. The direction of **q** and the position of the beam stop (BS) remain unchanged. Thus by moving the cell as shown the shear field can be rotated, allowing different orientations of particles with respect to the shear field to be investigated. (b) Schematic diagram of the Couette cell. Only the particles in an orientation in which the Bragg condition is met will diffract.

against shear rate, it shows that the sample is shear thinning at all shear rates investigated.

C. Neutron diffraction

Neutron diffraction measurements were made on the instrument D20, a diffractometer at the high flux reactor of the ILL, Grenoble, France [28]. It is equipped with a large detector covering an angular range of 160°. Shear was imposed on the samples in a purpose built Couette shear cell. The cell was constructed of aluminum but was varnished with a thin layer of poly (methyl methacrylate) to avoid contamination of the sample with any Al^{3+} ions. This cell had a hollow center so that by placing a beam stop within the stator, in the path of the beam, the scattering from just one point in the shear flow could be observed. The orientation of the flow field with respect to the incident beam was altered by placing the shear cell in such a way that the beam was incident on the cell at different angles as illustrated in Fig. 2(a). The constraints allowed that the Couette cell must remain vertical and at the geometry of D20 meant only that diffraction with the momentum transfer vector **q** in the flow-gradient plane could be investigated.

The diffraction technique used to measure the orientation distribution of particles has been described previously [17,18]. The intensity of a diffracted peak is proportional to the number of plates in the illuminated volume in the correct orientation to diffract as illustrated in Fig. 2(b).

Two diffraction peaks were used: the (001) peak, which is a reflection from atomic planes in the plane of the platelike particles, and the (100) peak, which is a reflection from atomic planes perpendicular to the plates. The scattering vector **q** for the (001) peak therefore lies in the direction of the plate normal. The (100) peak gives complementary information from the scattering vector that lies in the plane of the particles. The intensity of these peaks, and the background at the position of the peaks, was measured by fitting a Gaussian with a background to the measured scattering pattern. The background was primarily due to the hydrogen present in the dispersing media and the particles, and so was proportional to the volume of sample illuminated. Hence the integrated intensity under the fitted Gaussian was scaled by the background to account for changes in the illuminated volume and absorption, and was then taken to be proportional to the number of particles in the correct orientation to diffract.

D. Small-angle neutron scattering

Small-angle scattering measurements were made at the NIST Center for Neutron Research with the NG3 30 m SANS camera [29]. In order to cover an adequate range of momentum transfer vector **q** $[=4\pi/\lambda \sin(\theta/2)]$ with wavelength λ and scattering angle θ, two different configurations of sample to detector distance, collimation, and wavelength were used. The samples were sheared in a fused silica Couette cell [30]. It was possible to work with incident illumination in two directions: in the gradient direction, giving scattering patterns in the flow-vorticity plane, and in the flow direction, giving patterns in the gradient-vorticity plane. The bulk of the static inner cylinder prevented measurements at intermediate positions. Data for the empty cell were subtracted and the results normalized for relative detector efficiency using standard procedures [31]. The absolute intensities of the patterns in the flow-vorticity plane were determined by comparison with scattering from standard samples at each instrument configuration. The intensities of the patterns in the gradient-vorticity plane were not normalized in this way, because in this geometry the path length is long and not constant across the illuminated volume. Instead, the data in the gradient-vorticity plane were normalized by scaling the patterns so that the scattering in the vorticity direction matched that measured in the flow-vorticity plane.

IV. RESULTS AND DISCUSSION

A. Phase transition under steady shear

A sample containing 0.02*M* added NaCl at a particle weight fraction of 0.614 was investigated. At this concentration, the sample would phase separate into 67.4% columnar phase and the rest into the less ordered phase, if left to equilibrate for a number of days. The intensity of the (001) reflection from this sample was measured at a number of shear rates and is shown in Fig. 3. At high shear rates, the plates align with normals in the gradient direction (peak at 0°). However, at lower shear rates, the plates align with normals at 20° to the flow direction in the compressional quadrant (peak at 70°).

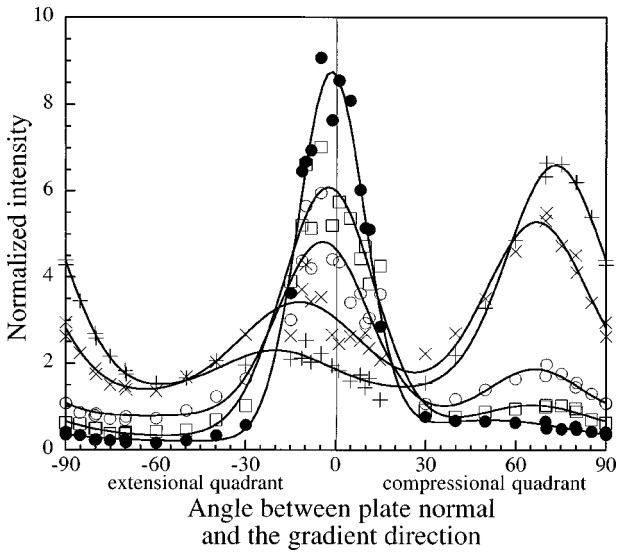

FIG. 3. Normalized diffracted intensity from a sample that would separate into 67.4% columnar phase and the rest into the less ordered phase if left for a number of days. The normalized intensity of the (001) reflection is given as a function of the angle between **q**, which is also the plate normal, and the gradient direction. The angle is zero in the gradient direction and positive in the compressional quadrant. The plot shows the variation between the gradient and flow directions at five shear rates: +, 0.6 s^{-1}; ×, 3.1 s^{-1}; ○, 9.7 s^{-1}; □, 22 s^{-1}; and ●, 67 s^{-1}. Lines have been drawn through the points to aid the eye.

Figure 4 shows the intensity profile for the (100) peak with angle. The intensity of the (100) diffraction peak corresponds to the integral of the number of particles oriented with normals perpendicular to **q**. As the shape of the intensity profile from the (100) peak is very similar to that from the (001) peak, this shows that the primary features of the orientation distribution function are those observed in the gradient-flow plane. Measurements were made for sufficient time so that curve fitting could give normalized intensities to typically a few percent accuracy. Within experimental error, similar data was also obtained for other Bragg peaks.

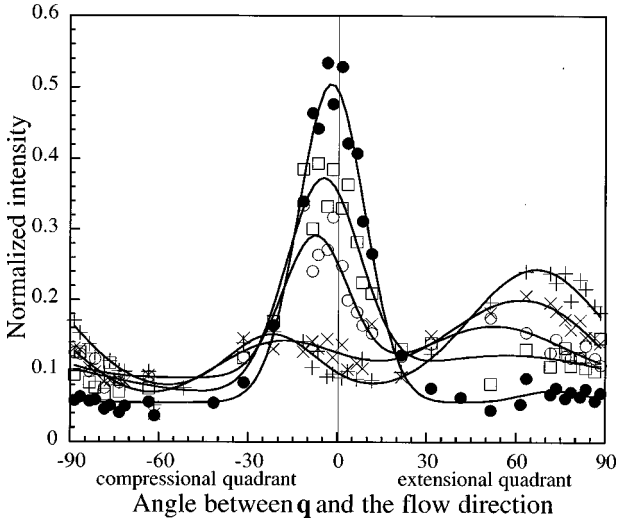

FIG. 4. Normalized intensity for the (100) reflection as a function of the angle between **q** and the flow direction from a sample that would separate into 67.4% columnar phase and the rest into the less ordered phase if left for a number of days. The angle is zero in the flow direction and positive in the extensional quadrant. The plot shows the variation between the gradient and flow directions at five shear rates: +, 0.6 s^{-1}; ×, 3.1 s^{-1}; ○, 9.7 s^{-1}; □, 22 s^{-1}; and ●, 67 s^{-1}.

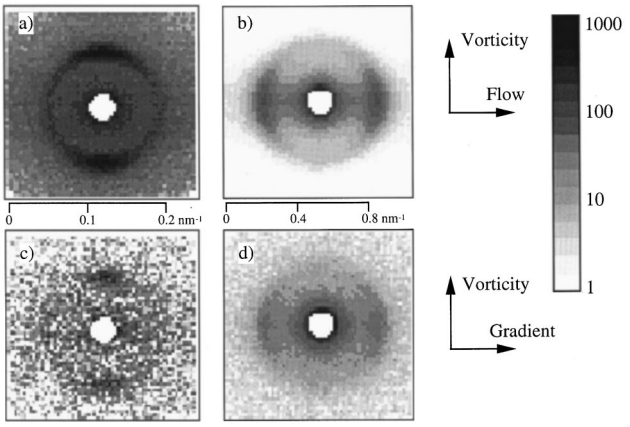

FIG. 5. SANS patterns from a sample that would separate into 70.2% columnar phase and the rest into the less ordered phase if left for a number of days, at a shear rate of 0.1 s^{-1}. (a) small **q** range; (b) large **q** range; beam incident radially on the Couette cell. (c) small **q** range; (d) large **q** range; beam incident tangentially on the Couette cell.

A very similar sample, containing 0.025*M* added NaCl and with a particle weight fraction of 0.625 was investigated using SANS. This sample would phase separate into 70.2% columnar phase and the rest into the less ordered phase, if left to equilibrate for a number of days. It was subjected to a number of shear rates, and the scattering profiles from two of these shear rates at two instrument configurations and both incident beam directions are shown in Figs. 5 and 6. From vertical and horizontal ±15° sectors of the patterns, the radial averages in Figs. 7(a) and 7(b) were obtained for the two shear rates. Each curve corresponds to an orthogonal direction in the sample.

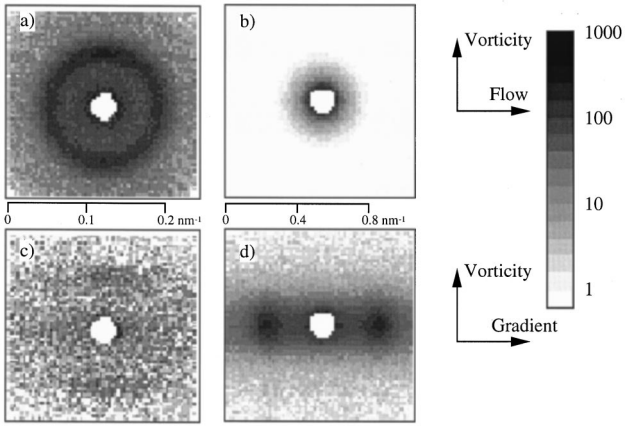

FIG. 6. SANS patterns from a sample that would separate into 70.2% columnar phase and the rest into the less ordered phase if left for a number of days, at a shear rate of 1000 s^{-1}. (a) small **q** range; (b) large **q** range; beam incident radially on the Couette cell. (c) small **q** range; (d) large **q** range; beam incident tangentially on the Couette cell.

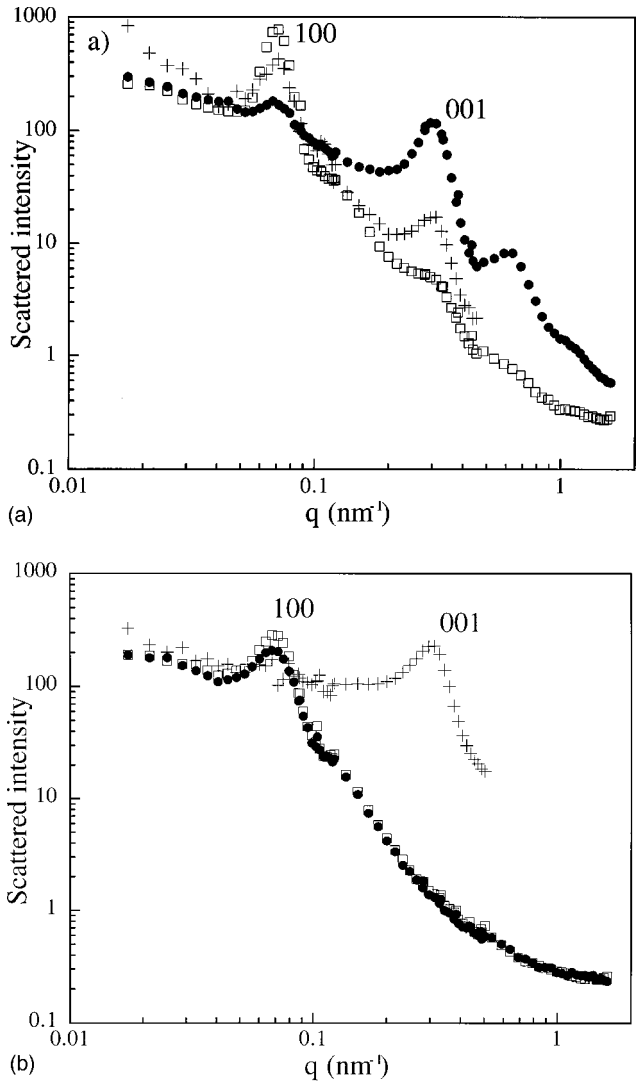

FIG. 7. Radial sectors ($\pm 15°$) of SANS patterns in the ● flow, □ vorticity, and + gradient directions from a sample that would separate into 70.2% columnar phase and the rest into the less ordered phase if left for a number of days. (a) 0.1 s^{-1}; (b) 1000 s^{-1}.

The scattering patterns display distinct peaks at two very different ranges of momentum transfer vector, **q**. The first, labeled 100, is at a value of **q** that corresponds to a distance similar to a plate diameter. The second, labeled 001, corresponds to a distance similar to the thickness of a plate and the polymer layer on its surface. To avoid confusion, the small-angle peaks corresponding to interparticle structure are indexed without brackets, i.e., 100, 001, etc., while the wide-angle peaks used to determine orientation of the individual crystalline particles (described above) are indexed with brackets (100), (001), etc.

The data for particle orientation (Figs. 3 and 4) show that at high shear rates, plate normals align in the gradient direction, and at low shear rates they align at 20° to the flow direction. Two observations can be made about this transition. The first is that as the sample moves from one direction of alignment to the other, the direction of orientation does not vary continuously but decreases in one direction while it increases in the other. This behavior is analogous to that of a phase transition rather than a continuous modification of a single phase. However, it should be noted that as a sheared system is not in equilibrium, a phase transition in the traditional sense cannot exist. The second observation is that this ''phase transition'' is not sharp, but rather occurs over a range of shear rates. This suggests that at intermediate shear rates two different shear-induced structures coexist, implying a shear-induced ''phase separation.''

Within a region of coexistence between two ''phases,'' the sample might be expected to band into layers of different phases that then shear at different rates. This shear banding has been observed by Pignon *et al.* [22], who describe planes normal to the gradient direction as might be expected for materials with a sharp change in viscosity. If the two phases were to have equal particle concentrations, then over the strain rates of the phase separation regime, the stress would remain constant. However, it is unlikely that the two phases would coexist at the same particle density. Since the total particle density in the system is constant, as the fraction of each phase present varies, the concentration of each phase would also change. The viscosity would then not remain constant across the region of phase separation. The rheology measurements on the nickel (II) hydroxide dispersion shown in Fig. 1 indicate a transition at a shear rate of 2 s^{-1}. The stress increases after this point, indicating that the higher shear rate phase is at a slightly lower concentration. As the shear rate is increased in the phase separation regime, the concentration of both phases must increase slightly.

The small-angle scattering also reflects this phase transition. Figure 7(b) shows that at 1000 s^{-1} the flow and vorticity directions both show a 100 peak, but almost no evidence of a 001 peak. In sharp contrast to this, the gradient direction shows almost no 100 peak but a very strong 001 peak. This suggests that spacings associated with the diameter of the particles are in the flow and vorticity directions, while spacings associated with the thickness of the particles are found in the gradient direction. Figure 7(a) shows that at 0.1 s^{-1} the scattering is quite different: the 100 peak is very small in the flow direction while the 001 peak is stronger. In the gradient and vorticity directions, the 100 peak is stronger and the 001 peak is weaker. This suggests that spacings associated with the diameter of the particles are in the vorticity and gradient directions, while spacings associated with the thickness of the particles are found in the flow direction. The contrast between the different directions is not as sharp as it was in the case of the 1000 s^{-1} flow. The 001 peak arises from a direction normal to the plates, and so should only appear in one direction in reciprocal space. The 001 peak is very strong in the flow direction; however, there is also a significant component of this peak in the gradient direction. These changes were reversible; measurements on increasing and decreasing shear rate were identical within statistical errors.

B. Structure of the ''phases'' at low and high shear rates

Columnar and layer structures are two possible simple liquid crystalline structures that could be supported by densely packed discs. The diffraction measurements indicate that at low shear rates the plates are oriented with their normals in the compressional quadrant, at 20° to the flow direction. The spatial arrangement of the particles in the structure at low shear rates can be deduced from the SANS measure-

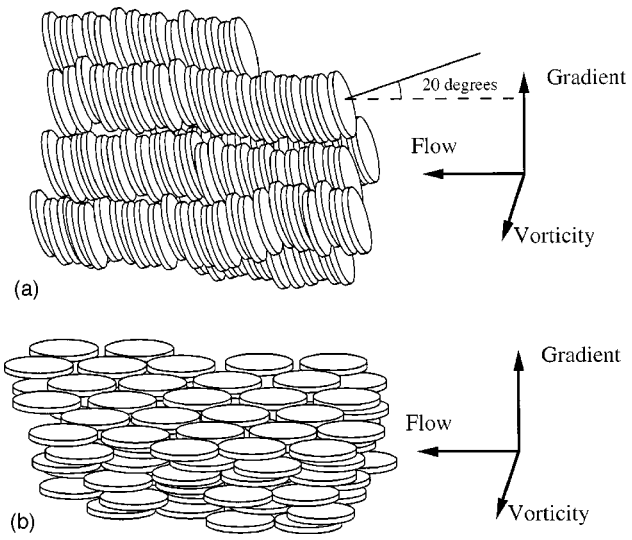

FIG. 8. Schematic diagram of the proposed structure at (a) low shear rates and (b) high shear rates.

ments shown in Figs. 5 and 7(a). A layered structure would be destroyed by the shear unless the flow direction was in the plane of the layers. The interlayer spacing in such a structure would result in a strong 100 peak in the gradient direction [Fig. 5(c)], which is clearly not present. An alternative structure would be a tilted columnar phase, where the columns lie along the flow direction while the particles are tilted by 20°. In this orientation, the columnar phase would not be destroyed by the shear because the columns of particles could slide along each other. A schematic diagram of this structure is shown in Fig. 8(a). This structure is also what one might expect intuitively, as under static conditions the particles form a columnar phase [14], and so the shear at low rate has simply aligned the static structure. Since the particles are unable to tumble in the flow, they have simply tipped until their rotation has been impeded by the next particle in the column.

The weak 001 peak observed in the gradient direction and the corresponding reduction in the 100 peak in the gradient direction and the small 100 peak in the flow direction Fig. 7(a)] suggest that some particles are oriented with normals in the gradient direction. This could be due to columns occasionally tumbling in the flow-gradient plane, though this would be unlikely to produce sufficient correlation between columns to give a 100 peak in the flow direction. Alternatively, it could be due to particles near the surface of the cell aligning with the surface. This kind of boundary effect would not be unprecedented, as colloidal crystals of spheres have been observed to orient at flat surfaces [32]. X-ray studies of the flow of clay particles in a pipe have also indicated that orientation parallel to a wall can be dominant over flow alignment [33].

Other structures are conceivable where the structure is continually broken and reformed by the flow, such as one in which the columns lie in the compressional quadrant. Such dynamic structures might be able to form; however, it is unlikely that they would produce structures ordered enough to produce the SANS peaks observed. The only structure that would satisfy all the criteria is the tilted columnar structure illustrated in Fig. 8(a).

In the high shear state, the plate normals are in the gradient direction. As described above for the low shear phase, either columns or layers of particles must lie normal to the gradient direction to prevent the shear field from destroying the structure. The small-angle scattering shows a strong 001 peak in the gradient direction [Figs 6(d) and 7(b)], suggesting that the particles are in layers normal to the gradient direction. A schematic diagram of this structure is shown in Fig. 8(b). Under shear these layers would slide over each other. This structure is also what one might intuitively expect, as it has been observed under a number of conditions that shear encourages plate-shaped particles to lie with their normals in the gradient direction. A layered structure such as this is the simplest structure that would allow the plates to lie in this orientation under shear and maintain the high level of positional order demanded by the high concentration of the plates.

These structures are also supported by the peak intensities in the small-angle scattering pattern. Following the arguments on positional disorder presented by Guinier [34], the lack of correlation between columns in a columnar phase would be represented in reciprocal space by the 001 peak being smeared out into a plane, normal to the columns. This plane should appear as a vertical line with a reduced intensity on Fig. 5(b). This reduction in intensity can be observed, as the 001 peak in the flow direction for the low shear phase [Fig. 7(a)] is weaker than the 001 peak in the gradient direction in the high shear phase [Fig. 7(b)]. If the 001 reflection in the flow direction in Fig. 5(b) is compared to that in the gradient direction in Fig. 6(d), it can be seen that the peak in Fig. 5(b) is smeared out in the vorticity direction. However, due to the anisotropy of the particles, the form factor causes the peak intensity to decay very quickly along this direction, so it does not appear as a uniform line.

Similarly, the loss of correlation between layers in a layer phase would be represented in reciprocal space by the 100 peak being smeared out into a line normal to the layers. This line should have a lower intensity than the diffraction point from a structure with no such loss of correlation. This reduction in intensity can be observed, as the 100 peak in the flow and vorticity directions from the high shear phase [Fig. 7(b)] is weaker than the 100 peak in the gradient and vorticity directions in the low shear phase [Fig. 7(a)]. The line would be expected to appear as a horizontal line on Fig. 6(c). The pattern suggests such a line; however, the noise in the data and the effect of the form factor makes it difficult to be certain of such an observation. The slight anisotropy in the 100 ring in Fig. 6(a) suggests that there might be some residual correlation between layers in the vorticity direction, but the intensity variation is small, so any corresponding correlation would be slight.

C. Other shear rates and concentrations

So far, only two shear rates have been discussed. Figure 9 shows the peak intensities in the flow and vorticity directions for both the 100 and the 001 peaks over a range of shear rates. Between shear rates of 0.1 and 1 s^{-1}, the order observed at low shear increases such that diffraction peaks are strongest around 1 s^{-1}. This suggests that in this region the imposed shear tends to increase the positional order. The

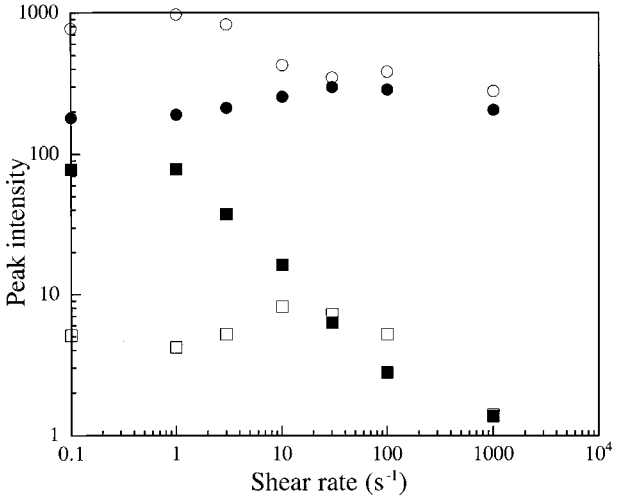

FIG. 9. Variation of the SANS peak intensities with shear rate for a sample that would separate into 70.2% columnar phase and the rest into the less ordered phase if left for a number of days. ●, 100 peak in the flow direction; ○, 100 peak in the vorticity direction; ■, 001 peak in the flow direction; □, 001 peak in the vorticity direction.

sample then undergoes the transition between 1 and 30 s^{-1}. In the range of shear rates between 100 and 1000 s^{-1}, the intensity of all the peaks decreases, suggesting that the positional order in the layer structure is destroyed.

The variation of peak intensities with shear rate for two more dilute samples is shown in Figs. 10(a) and 10(b). The points are averages of two measurements, one taken as the shear rate was increased and the other taken as the shear rate was decreased. These plots show the same features as the more concentrated sample, although the magnitudes of the changes are reduced. This suggests that the degree of order is reduced, or that two regions exist—an ordered region and a disordered region—and that at lower concentrations, less sample is in the ordered state.

These observations are also supported by diffraction measurements made on more dilute samples. Two samples at weight fractions of 0.606 and 0.579 gave alignment as shown in Fig. 11. These samples would phase separate into 54% and 20%, respectively, of the columnar phase, while the rest would remain in the less ordered phase, if left to equilibrate for a number of days. Figure 11 shows that samples toward the dilute end of the phase coexistence region display less alignment under shear. However, the directions of ordering and the shear rates at which they are observed appear to remain essentially unaltered.

The observed shear-induced phase transition illustrates a competition between the effect of flow on a single particle and the entropic gain of the free volume associated with the columnar phase over that of a layered structure. High shear favors the alignment of a single particle with its normal in the gradient direction. The free volume associated with the particles being in the columnar phase favors shear in sliding columns of particles. At low shear rates the increased entropy of the columnar phase dominates, giving an aligned columnar phase, while at high shear rates the effect of the flow on the individual particles is strong enough to make the layer phase more favorable than the columnar phase.

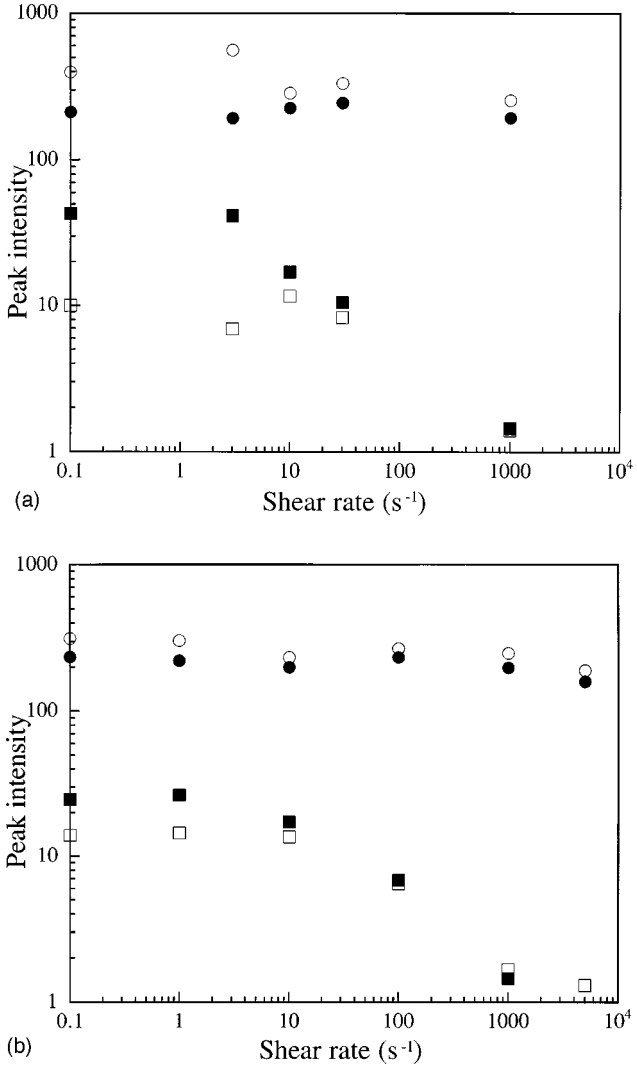

FIG. 10. Variation of the SANS peak intensities with shear rate for a sample that would separate into (a) 53.1% of the columnar phase and (b) 40.5% of the columnar phase. ●, 100 peak in the flow direction; ○, 100 peak in the vorticity direction; ■, 001 peak in the flow direction; □, 001 peak in the vorticity direction.

Dispersions of more polydispersed plate-shaped particles have shown some similar features to those described here. Under shear, kaolinite plates typically move from a disordered state at rest to align with normals in the gradient direction at high shear rates; however, the low polydispersity and controlled particle interactions produce positional order at both low and high shear rates.

D. Static structure after shear

The sample with weight fraction of 0.614 and with 0.02*M* added NaCl was investigated using neutron diffraction. This sample would phase separate into 67% columnar phase and the rest into the less ordered phase, if left to equilibrate for a number of days. This sample was sheared for a number of hours at different shear rates. After each period of shear, the shear was then stopped and the sample was allowed to relax for a further period of a few hours. During the periods of shear and relaxation, the normalized intensities from the (001) and (100) wide-angle scattering peaks were measured.

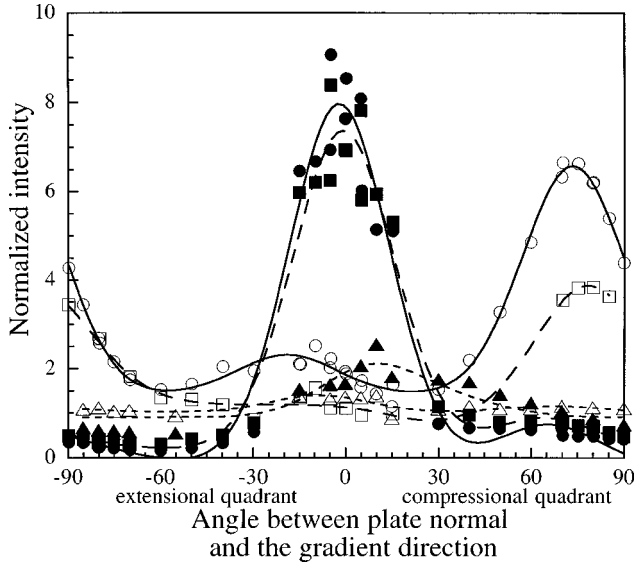

FIG. 11. Normalized intensity for the (001) reflection as a function of the angle between **q** and the gradient direction. The angle is zero in the gradient direction. The plot shows the variation in the density of normals between the gradient and flow directions for three samples that would separate into 67% (○, 0.6 s^{-1}; ●, 67 s^{-1}), 54% (□, 0.6 s^{-1}; ■, 67 s^{-1}) and 20% (△, 0.6 s^{-1}; ▲, 67 s^{-1}) columnar phase, and the rest the less ordered phase if left for a number of days.

The (001) peak has a scattering vector coincident with the normals to the plates and so simply defines their orientation. Complementary data for a scattering vector **q** in the plane of the plates comes from the (100) peak. These are shown for two different shear rates in Figs. 12(a) and 12(b). After shear at either high or low shear rates, the direction of the alignment of the particles does not change significantly on stopping the shear, but the extent of alignment is increased.

SANS measurements were made from the similar sample, at a weight fraction of 0.625 with 0.025*M* added NaCl. This sample would phase separate into 70% columnar phase and the rest into the less ordered phase, if left to equilibrate for a number of days. Figure 13 shows the scattering patterns in the vorticity-gradient plane after shear rates of 0.1 and 1000 s^{-1}, compared to those observed under flow. The scattering pattern after shear 0.1 s^{-1} appears very similar to that observed under flow. The pattern measured at rest after 1000 s^{-1}, however, shows a very marked change. The ring from the 100 diffraction peak, corresponding to a distance that is approximately the diameter of the particles, divides into six peaks when the shear is stopped.

The degree of orientational order is much greater at rest after shear at any speed than during the shear, and the orientation does not significantly alter direction. In order to determine the structure of the crystal after the shear field is removed, the small-angle scattering from the samples under shear and at rest must be compared. Figure 14 compares the variation of scattered intensity with **q** in a direction approximately in the plane of the particles, for the sample during and after high and low shear rates. The 100 peak in the vorticity direction from the sample undergoing shear at 0.1 s^{-1} is very similar in intensity and width to the peak in the vorticity direction from the static sample after shear at 0.1 s^{-1}. This indicates that there is no substantial change in

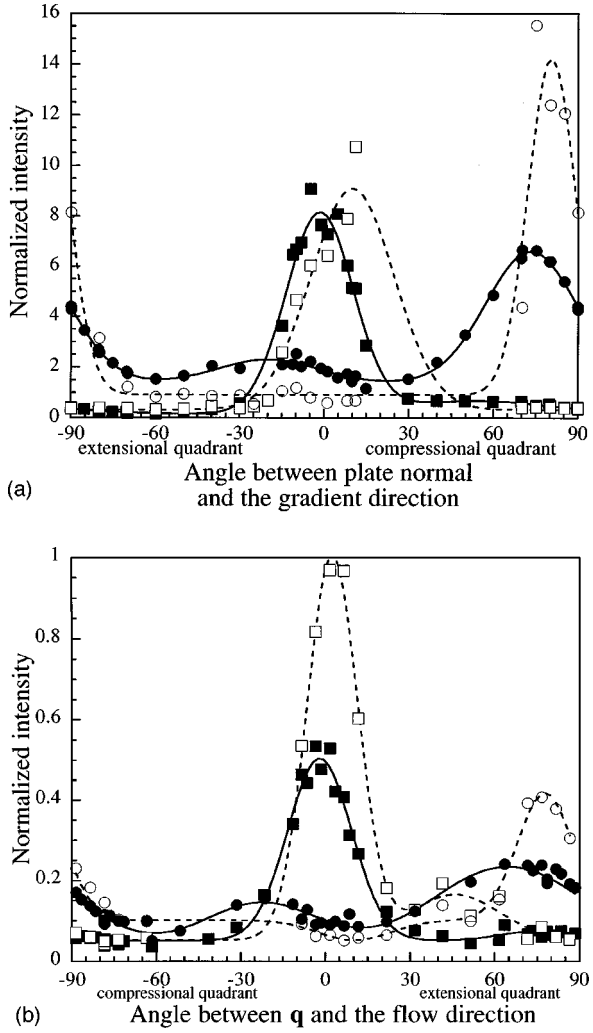

FIG. 12. Normalized diffracted intensity of the (a) (001) reflection and the (b) (001) reflection as a function of angle in the gradient-flow plane, from a sample that would separate into 67% columnar phase, the remainder forming the less ordered phase if left for a number of days: ●, during shear of 0.6 s^{-1}; ○, after shear of 0.6 s^{-1}; ■, during shear of 67 s^{-1}; and □, after shear of 67 s^{-1}. Lines have been drawn through the points to aid the eye.

positional order when the sample is stopped after low rates of shear. Hence the structure after the sample is subjected to low shear rates is columnar.

The average of the intensity of the 100 peak around the hexagonally ordered ring seen in the sample after shear at 1000 s^{-1} [Fig. 13(b)] is plotted in Fig. 14. This average has a very similar shape and intensity to that from the sample during and after shear at low rates. This similarity indicates that the structure after high shear is also columnar. The hexagonal pattern of peaks indicates that after high rates of shear the sample consists of a number of oriented domains or a single domain. The curve in Fig. 14 from the sample under shear at 1000 s^{-1} is in stark contrast to the other three curves. The lower intensity of the 100 peak is due to the lack of correlation between particles in different layers within the layered structure formed under conditions of high shear as described above. This means that the sample moves from a layered structure into a columnar phase after high shear.

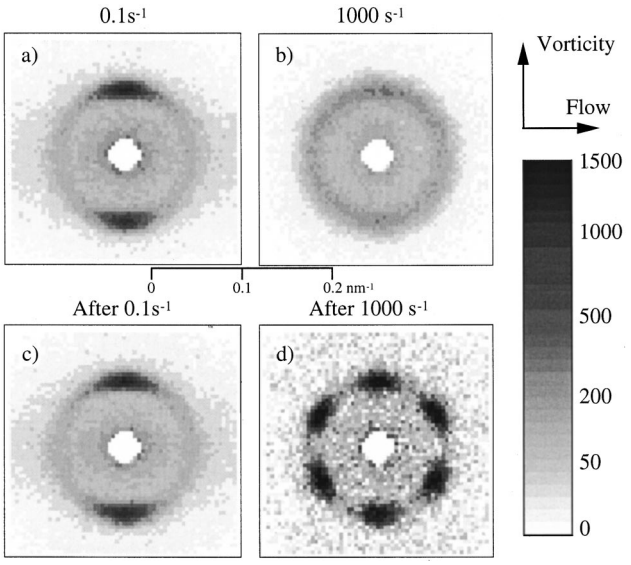

FIG. 13. SANS patterns from a sample that would separate into 70% columnar phase and the remainder into less ordered phase if left for a number of days: (a) during a shear of 0.1 s^{-1}, (b) during a shear of 1000 s^{-1}, (c) static after a shear rate of 0.1 s^{-1}, (d) static after a shear rate of 1000 s^{-1}. The visible peaks are the hk0 peaks. The 001 peaks relate to a smaller distance in real space and so are at larger angles than those investigated with this instrument configuration.

E. Dynamics of relaxation

Both the NG3-SANS instrument and the diffractometer D20 were equipped with data acquisition systems suitable for repeated accumulation of data from cyclic processes. This permits data with adequate statistical accuracy to be collected on fast processes that are repetitive. In this way, microscopic dynamic processes in the millisecond time range can be studied [35]. The time evolution of the particle orientations in the sample at a weight fraction of 0.614 was also

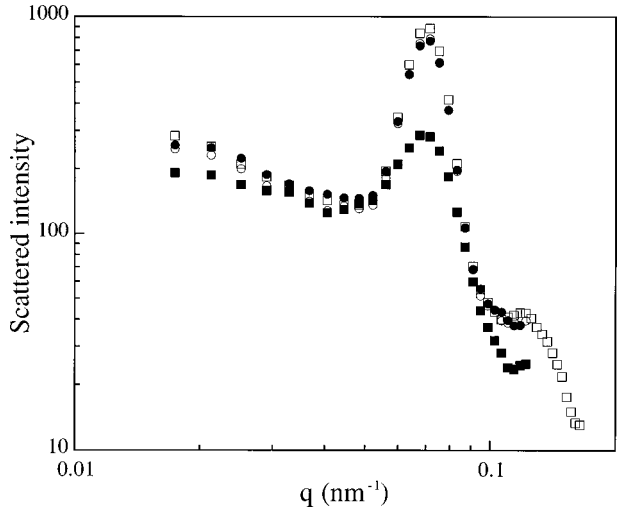

FIG. 14. Radial plots from 15° sectors of the SANS patterns shown in Fig. 13, showing the 100 peak. ■, scattering in the vorticity direction at 1000 s^{-1}; ●, scattering in the vorticity direction at 0.1 s^{-1}; □, average of the scattering in the vorticity-flow plane after shear at 1000 s^{-1}; ○, scattering in the vorticity direction after shear at 0.1 s^{-1}.

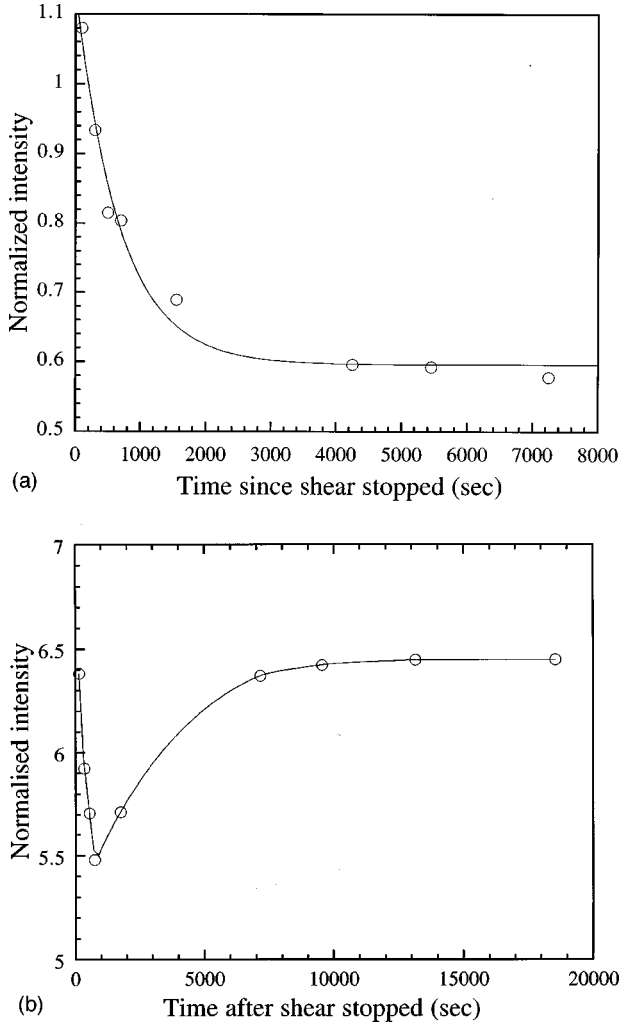

FIG. 15. Variation of diffracted intensity for the (001) reflection from a sample that would separate into 67% columnar phase and the remainder into the less ordered phase if left for a number of days, as a function of time. The intensity is proportional to the number of plates with normals in a direction in the flow-gradient plane at 1.2° to the gradient direction (a) after a shear rate of 0.6 s^{-1} was removed and (b) after a shear rate of 67 s^{-1} was removed.

investigated. This was done by following the variation in the number of particles oriented at 1.2° to the gradient direction using the (001) wide-angle diffraction peak. Figure 15(a) shows how, after a low rate of shear (0.6 s^{-1}), the intensity in this direction decays as the particles increase their alignment with normals at 20° to the flow direction. Figure 15(b) shows how, after a high rate of shear (67 s^{-1}), the orientational order does not simply increase as would be expected, but decreases to a minimum after the first 10 min before subsequently increasing.

The time evolution of the SANS pattern from the sample at a weight fraction of 0.625 after shear at 1000 s^{-1} was also investigated. Dynamic data acquisition with cycles of 5 s constant shear and 5 s rest and also cycles of 60 s constant shear and 45 s rest allowed the structural order after flow at 1000 s^{-1} to be investigated as shown in the sequence of SANS images in Fig. 16.

After the slow shear (0.1 or 0.6 s^{-1}), the degree of orientational order simply increases as the particles settle into

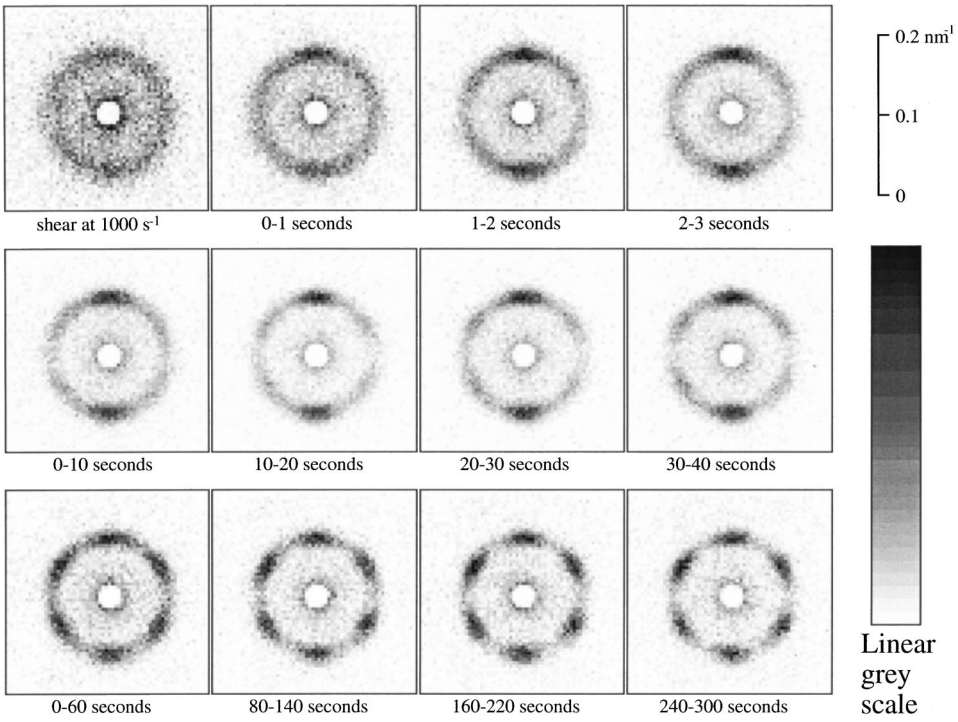

FIG. 16. Time evolution of small-angle scattering patterns in the flow-vorticity plane after a shear of 1000 s^{-1} is stopped. The sample is at a concentration that would separate into 70% columnar phase and the remainder into the less ordered phase if left for a number of days. The visible peaks are the hk0 peaks. The 001 peaks relate to a smaller distance in real space and so are at larger angles than those investigated with this instrument configuration. The first plot is shear at 1000 s^{-1}. The other plots are labeled with the time over which the measurement was taken. The gray scale has been adjusted on each figure to accommodate the growing hexagonal peaks.

equilibrium positions. The decay in the density of particles oriented perpendicular to the preferred direction is roughly exponential, with a decay time of around 680 s. This time gives an insight into the mechanism of relaxation. If a particle rotated independently of its neighbors, then rotational diffusion would be at the same rate as for an isolated particle dispersed in water. In this case the rotational diffusion coefficient would be 640 s^{-1}, which would give a characteristic decay time of a few milliseconds. However, if cooperative motion is required for the particle to rotate, then the viscosity of the dispersion gives a better estimate of the expected rotational diffusion coefficient than using the viscosity of water. The viscosity of the concentrated dispersion is around 10^5 times larger than that of water, which would give a decay time of a few hundred seconds. This estimate is in keeping with the observed decay time, suggesting that the reorientation within the sample could be modeled by a particle diffusing in a medium with the same viscosity as the sample. This suggests that this reorientation involves some cooperative motion of particles rather than purely local motion within a preferred site in an ordered structure.

After shear at high rates, the relaxation process is less simple. As soon as shear is stopped, the 100 peak in the vorticity direction starts to grow considerably while there is only small growth in the other 100 peaks. This indicates that the positional order between particles in the vorticity direction is achieved before positional order in the flow direction. This suggests that the sample, after approximately 40 s, has an intermediate structure as shown in Fig. 17. This intermediate structure allows the sample to move from a layer phase to a columnar phase without having to pass through the crystalline phase that is not favored by entropy with order in all three directions. The other peaks then grow to give the final SANS pattern after about 200 s, which is characteristic of the hexagonal arrangement of columns observed at long times as discussed earlier.

The diffraction measurements show that throughout this period the orientational order decreases up until around 800 s after the shear is stopped. The decrease in orientational order and the rearrangement of the structure occur on similar time scales, suggesting that the positional structure alters at the expense of some orientational order. Once the final positional structure has been achieved, the orientational order then increases. This increase in orientational order is roughly exponential with a decay time of 2400 s. It is not obvious why this relaxation time for the alignment of the particles should be longer after shear at high rates than it was after lower shear rates. The difference in the shear history may well give rise to a residual difference in the positional order present; for example, the uniformity of the particle separation may be different. These subtle differences may then give rise to a different mechanism for reorientation, such as one that involves a higher degree of cooperative motion. The model of using the bulk viscosity to calculate a relaxation

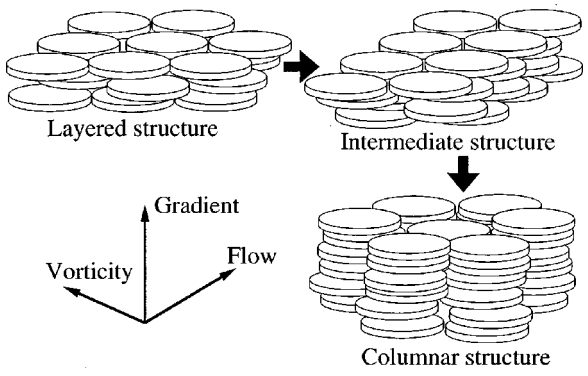

FIG. 17. Schematic drawing of the progression of the positional structure, from the layered structure present at high shear, via a structure with layers of particles normal to the vorticity direction, to the final columnar structure.

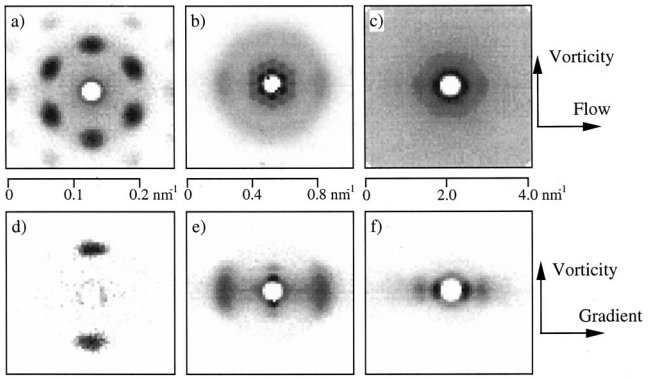

FIG. 18. SANS observed at three **q** ranges, after oscillatory shear was removed. The intensity shading shows steps on a linear scale, and the range has been adjusted on each pattern to bring out the features present.

time is very crude and so cannot account for differences such as these.

F. Structure after oscillatory shear

A more dilute sample with a weight fraction of 0.62, which separated into 53% of the columnar phase and the rest into the less ordered phase if left for a number of days, was also investigated. Under shear, it displayed similar characteristics to the more concentrated sample as described in the previous paper. However, after high shear was removed it did not show hexagonal order in the 100 SANS peak. This does not mean that the columns are not hexagonally packed, but that the orientation of this packing is not constant across the sample. Hence the sample that would separate into 70% columnar phase showed the hexagonal peaks after high shear, whereas the sample that would separate into a 53% columnar phase did not. The sample phase separates, as described previously [14], by droplets of the columnar phase forming in a matrix of the disordered phase. 70% volume fraction is above the maximum packing fraction for uniform spheres, so it could be that at this concentration the more ordered phase is forced to form a space spanning structure, which causes the orientation of the hexagonal packing of the columns to also be space spanning. At 53%, however, droplets of the columnar phase can remain isolated, allowing each droplet to have a different orientation of the hexagonal packing.

This sample was then investigated by SANS under oscillatory shear at a frequency of around 5 Hz and with a strain amplitude of about 1. Under shear, the sample displayed a SANS pattern with a 100 ring in the flow-vorticity plane with very slight hexagonal ordering. Figure 18 shows the small-angle scattering patterns observed after shear was stopped. The order displayed is greater than even that observed with a more concentrated sample after a high continuous shear rate. The high degree of order observed shows that oscillatory shear is very good at producing long-range order, although the highly ordered structure only forms after the shear is removed.

V. CONCLUSIONS

A concentrated colloidal dispersion of monodispersed plates of nickel (II) hydroxide has been studied under shear. At low shear rates the columnar phase that exists at rest is aligned with columns in the flow direction. The shear also orients the particles with their normals at 20° to the flow direction in the compressional quadrant. There is evidence that at the boundaries, the particles may be aligned in an orthogonal orientation by the surface of the shear cell. As the imposed shear rate is increased, the sample undergoes a transition to a layer ''phase,'' in which the layers and the particles are oriented with normals in the shear gradient direction. The region of transition between these two phases is observed to be between 1 and 30 s^{-1}. At higher shear rates, the amount of order is reduced, suggesting shear-induced melting. The clear transition between two distinct ordered structures is unusual and has not been observed previously. The monodispersity of the particles in the dispersion may accentuate the ability to form highly ordered phases.

When shear is removed from a concentrated dispersion of the platelike particles, the particles change into or remain in a columnar structure. This structure is oriented so that the particles do not change their direction of alignment when the shear field is removed. The degree of orientational order observed is greater after shear than it is during shear. After shear at low rates (0.1 or 0.6 s^{-1}), there was no measurable change in the positional order, and the orientational order increased with a characteristic time of 680 s. This time is the same order of magnitude as the inverse rotational diffusion coefficient for a single particle in a medium of the viscosity of the dispersion. At rest after shear at higher rates (1000 or 67 s^{-1}), the structure changes from a layered structure to a columnar structure. This positional change occurs via an intermediate structure with particles in layers normal to the vorticity direction. The orientational order decreases during the positional changes and then increases again with a longer characteristic time of 2400 s.

These results indicate that cooperative motion of the particles may be very important in determining the relaxation after shear. Alignment and reorientation may involve the motion of several particles or the annealing of defects in a structure rather than the simple reorientation of particles while in fixed lattice positions. The structural mechanism for motion depends in a complex way on shear as different strain histories may give rise to different structures with distinct mechanisms of relaxation. Diffraction and scattering techniques provide a unique probe for these phenomena as, unlike rheological measurements, they do not further perturb the structure during the investigation.

ACKNOWLEDGMENTS

We acknowledge the support of the National Institute of Standards and Technology, U.S. Department of Commerce, in providing SANS facilities used in this work. This material is based upon activities supported by the National Science Foundation under Agreement No. DMR-9423101. We are grateful to the Institute Laue Langevin for neutron diffraction time. We thank the UK EPSRC for financial support. Dr. Tania Slawecki assisted with the SANS measurements at NIST and Dr. Pierre Convert helped with the operation of the D20 diffractometer at the ILL. Dr. Martin Bates and Professor Daan Frenkel kindly provided copies of their manuscripts prior to publication.

[1] B. J. Ackerson and N. A. Clark, Physica A **118**, 221 (1983).
[2] S. Ashdown, I. Markovic, R. H. Ottewill, A. R. Rennie, P. Lindner, and R. C. Oberthür, Langmuir **6**, 303 (1990).
[3] H. Versmold, Phys. Rev. Lett. **75**, 763 (1995).
[4] R. H. Ottewill and A. R. Rennie, Int. J. Multiphase Flow **16**, 681 (1990).
[5] S. M. Clarke, A. R. Rennie, and R. H. Ottewill, Adv. Colloid Interface Sci. **60**, 95 (1995).
[6] L. B. Chen, C. F. Zukoski, B. J. Ackerson, H. J. M. Hanley, G. C. Straty, J. Barker, and C. J. Glinka, Phys. Rev. Lett. **69**, 688 (1992).
[7] Ch. Dux, H. Versmold, V. Reus, T. Zemb, and P. Lindner, J. Chem. Phys. **104**, 6369 (1996).
[8] D. M. Heyes and P. J. Mitchell, J. Non-Newtonian Fluid Mech. **68**, 101 (1997).
[9] R. C. Ball and J. R. Melrose, Physica A **247**, 444 (1997).
[10] J. F. Brady and J. F. Morris, J. Fluid Mech. **348**, 103 (1997).
[11] L. E. Silbert, J. R. Melrose, and R. C. Ball, Phys. Rev. E **56**, 7067 (1997).
[12] W. B. Russel, D. A. Saville, and W. R. Schowalter, *Colloidal Dispersions* (Cambridge University Press, Cambridge, 1989).
[13] A. B. D. Brown, S. M. Clarke, and A. R. Rennie, Langmuir **14**, 3129 (1998); **15**, 1594 (1999).
[14] A. B. D. Brown, A. R. Rennie, C. Ferrero, and T. Narayanan, Eur. Phys. J. **11**, 481 (1999).
[15] J. A. C. Veerman and D. Frenkel, Phys. Rev. A **45**, 5632 (1992).
[16] M. Bates and D. Frenkel (unpublished).
[17] S. M. Clarke, A. R. Rennie, and P. Convert, Europhys. Lett. **35**, 233 (1996).
[18] A. B. D. Brown, S. M. Clarke, and A. R. Rennie, Prog. Colloid Polym. Sci. **110**, 80 (1998).
[19] H. J. M. Hanley, G. C. Straty, and F. Tsvetkov, Langmuir **10**, 3362 (1994).
[20] J. D. F. Ramsey and P. Lindner, J. Chem. Soc., Faraday Trans. **89**, 4207 (1993); **90**, 2001 (1994).
[21] S. M. Jogun and C. F. Zukoski, J. Rheol. **43**, 847 (1999).
[22] F. A. Pignon, J. M. Magnin, and J. Piau, Phys. Rev. Lett. **79**, 4689 (1997).
[23] A. B. D. Brown, S. M. Clarke, and A. R. Rennie, J. Rheol. **44**, 221 (2000).
[24] F. M. van der Kooij and H. N. W. Lekkerkerker, J. Phys. Chem. B **102**, 7829 (1998).
[25] A. C. Branka and D. M. Heyes, J. Chem. Phys. **109**, 1 (1998).
[26] X. F. Yuan and M. P. Allen, Physica A **240**, 145 (1997).
[27] The sodium polyacrylate was supplied by Allied Colloids, called DISPEX N40, and had a nominal molecular weight of 3200.
[28] H. G. Büttner, E. Lelièvre-Berna, and F. Pinet, *Guide to Neutron Research Facilities at the ILL* (Institut Laue Langevin, Grenoble, 1997).
[29] C. Glinka, J. Barker, B. Hammouda, S. Krueger, J. Moyer, and W. Orts, J. Appl. Crystallogr. **31**, 430 (1998).
[30] G. C. Straty, H. J. M. Hanley, and C. J. Glinka, J. Stat. Phys. **62**, 1015 (1991).
[31] A. R. Rennie, in *Modern Aspects of Small-Angle Scattering*, edited by H. Brumberger (Kluwer Academic, Dordrecht, 1995), pp. 93–105.
[32] S. M. Clarke and A. R. Rennie, Faraday Discuss. **104**, 49 (1996).
[33] S. Bare, A. R. Rennie, J. K. Cockcroft, and S. L. Colston (unpublished).
[34] A. Guinier, *X-Ray Diffraction in Crystals, Imperfect Crystals, and Amorphous Bodies* (W. H. Freeman and Company, San Francisco, 1963).
[35] A. R. Rennie and R. C. Oberthür, Rev. Phys. Appl. **19**, 765 (1984).